Space-charge layers on Ge surfaces. I. dc conductivity and Shubnikov–de Haas effect

J. Binder,* K. Germanova,† A. Huber, and F. Koch
Physik-Department, Technische Universität München, 8046 Garching, Germany
(Received 1 March 1979)

We have prepared metal-insulator-semiconductor (*M-I-S*) structure for major symmetry planes of Ge. The samples are examined and characterized systematically by capacitance-voltage (*C-V*) and conductivity measurements [$\sigma(V)$ and $d\sigma/dV_g$]. Lacquer-coated specimens of (111) surfaces prepared in this work give a new period in the magneto-oscillation spectrum and thus resolve the question of "missing" electrons raised in the experiments of Weber *et al.* We determine the energy splitting of the two lowest electron subbands on (111) Ge and predict the occupancy of the lowest level of the threefold degenerate valleys for N_s above $\sim 1.0 \times 10^{12}$ cm^{-2}.

I. INTRODUCTION

The fact that Ge (111) surfaces in *M-I-S* (metal-insulator-semiconductor) structures could be prepared sufficiently well to show surface conductivity, magnetoquantum oscillations, and cyclotron resonance was demonstrated in the experiments of Weber *et al.*[1] This work had raised a disconcerting question. A single period of oscillation, indicative of a single occupied subband, was observed over the entire range of induced surface charge N_s ($N_s \leq 6.2 \times 10^{12}$ cm^{-2}). The observed cycloton mass m_c^* indicated a valley degeneracy of $g_v = 1$. Knowing this, the subband occupation was identified as *only* $\sim$20% of the charge N_s.

The missing charge could not reasonably be accounted for in Ref. 1. One expects for (111) Ge a system of electron subbands $n = 0, 1, 2, \ldots$ derived from the nondegenerate valley with large mass perpendicular to the surface. A second set of subbands, $n = 0', 1', 2', \ldots$ with higher energies, would come from the remaining three valleys. Weber *et al.*[1] assumed that the observed period originated from the $n = 0$ electrons. The possibility that a higher, say $n = 1$, subband gave rise to the oscillations while the remaining missing charge was contained in a poor-mobility $n = 0$ state was considered unlikely. It was argued that then, over the wide range of N_s studied, also oscillations from $n = 2$ electrons should have been observed. We have come to realize from a simple triangular-potential-well estimate, however, that the 0′ subband with its very high density of states would lie near the $n = 2$ level. This would lead to a pinning of the Fermi energy in the $n = 0'$ subband. No oscillations from the few $n = 2$ carriers would then be observed. This chain of reasoning led us to reexamine the possibility of the existence of a lower-lying, poor-mobility $n = 0$ subband.

To observe such a subband, better surface preparation would be required. It was thought that in particular the range of low N_s, where surface roughness scattering was not dominant and where the Mylar-foil covered samples had proved unreliable, needed further exploration. We have in the course of this work developed a lacquer-coating technique for Ge, which has resulted in a better and more stable interface. A new perspective on the subband occupation question came with the appearance of some extra structures for the lacquer-type samples. Figure 1 is a good indication of the progress that has been achieved in the work with Ge (111) surfaces. The extra peak proved later to be the decisive clue for the proper interpretation.

In the course of this work we have worked with *n*- and *p*-type materials, with very high purity samples

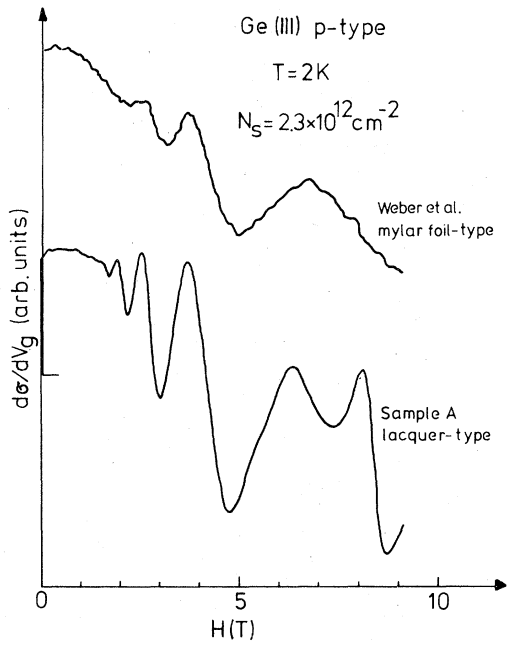

FIG. 1. Comparison of the magneto-oscillations in the differentiated conductivity for foil-type and lacquer-coated samples.

($N_{D,A} \sim 10^{11}$ cm^{-3}) and the conventional purity grades ($N_{D,A} \sim 10^{14}$ cm^{-3}). Different surface preparation procedures have been tried. All of this was in conjunction with systematic surface capacitance versus voltage (C-V) and surface conductivity analysis. We have raised the question of possible quantum effects in the magnetoconductivity of (100) and (110) surfaces.

After some experimental remarks in Sec. II we deal with C-V and conductivity characterization of the samples in Secs. III and IV. Section V gives the results of the Shubnikov-de Haas measurement. It is followed by a discussion of what these results imply for the subband energy structure of Ge in Sec. VI.

II. SOME EXPERIMENTAL REMARKS

Emphasis in this work was on the development of the surface preparation procedure and a systematic evaluation of the surfaces by C-V and conductivity measurements. Additional improvements on the microwave apparatus have simplified the measurement and improved the signal-to-noise ratio over that in Ref. 1.

Typical samples are x-ray oriented and cut from bulk material to the desired orientation [(100), (110), or (111)] and dimension $\sim 6 \times 7 \times 1.5$ mm^3. The sample surface is chemically lapped and polished. The best and most consistent results were obtained with the 1:50 mixture of NaOCl (~150 g/liter) solution and distilled water at 95 °C. Samples are polished under continuous motion for 1–2 hours. They are removed from the bath and washed in acetone. We have tried various forms of treatment after the polish. These included oxygen and inert-gas annealing, oxidation by dipping in boiling water, and aging under ambient conditions.

Quite good results were obtained with samples coated with the dielectric layer immediately after the polish and without additional treatment. Inert-gas annealing at 700 °C sometimes gave a slightly better surface. The diluted lacquer (Plastik 70, manufactured by Kontakt Chemie) is applied in a thinner of the type used in photolithographic applications. Typical lacquer thickness is 1–3 μm. Its dielectric strength when coated on polished Ge is ~100 V/μm.

For comparison we have made several samples with Mylar-foil insulators as described in Ref. 1. These "naked" samples generally had a higher density of interface states N_{ss} and tended to change with time. The lacquer-coated specimens were stable. For both the foil- and lacquer-type samples the induced surface charge per volt applied to the gate electrode is obtained from the measured capacitance C ($T \sim 4.2$ K). The gate electrode is a semitransparent layer of Ni-Cr (~50 Å thick, area 14.7 mm^2). The samples are labeled $A, B, \ldots, I$. Their orientation, doping, insulator, and surface treatment are listed in Table I.

Measurements of surface conductivity are made in a 14-GHz-microwave spectrometer in either a conventional reflection[2] or transmission configuration.[3] The sample is mounted horizontally across the waveguide. The microwave generator is an IMPATT diode with ~50-mW output. The straight transmission configuration is simpler to use because it does not require tuning of the magic-Tee bridge.

The microwave frequency ω is much less than the typical relaxation frequency of electrons on Ge surfaces. It follows that $\sigma(\omega) \simeq \sigma_0$. The fractional transmission T of a wave traversing a thin conducting layer is $T = 1/(1 + \frac{1}{2}f)^2 \simeq 1 - f$ with $f = 377\,\Omega/R_\square$ and $R_\square$ equal to the resistance per square of the layer in Ω. For even the best Ge surfaces $R_\square \geq 1000\ \Omega$. The fractional area of the waveguide cross section

TABLE I. Description of samples.

Samples	Doping	Insulator	Surface treatment
A (111)	$N_A \sim 10^{11}$ cm^{-3}	lacquer ~2 μm	NaOCl, tempered (700 °C, 1h)
B (111)			NaOCl
C (111)			modified CP-4[a]
D (111)	$N_A \sim 2 \times 10^{14}$ cm^{-3}	Mylar foil 3.5 μm	NaOCl
E (111)			
F (111)			
G (110)			
H (100)			
I (111)	$N_D \sim 2 \times 10^{14}$ cm^{-3}	lacquer ~2 μm	

[a]CP-4 is a mixture of one part hydrofluoric acid, one part glacial acetic acid, $1\frac{1}{2}$ parts concentrated nitric acid, and a few drops of liquid bromine per 50 cm^3.

covered by the surface layer is $\frac{1}{10}$. The observed and theoretically expected change in transmission is of the order of 4%, i.e., sufficiently small to be linearly proportional to the conductivity. The E field in the waveguide is linearly polarized parallel to the narrow face of the guide. A Hall field cannot exist in the given waveguide geometry. It follows that the absorption measured in a magnetic field is proportional to $\sigma_{xx}(H)$.

III. SAMPLE CHARACTERIZATION BY C-V MEASUREMENTS

The C-V relation is an indication of surface band bending and the existence of a charge layer at the surface. It can be used to identify the flat-band voltage V_{FB} and the inversion threshold V_T. Moreover it is a measure of the quality of surface preparation in that it gives the interface density of charge N_{ss}.

In order to measure and interpret the low T (4.2 K) C-V curve we make use of the understanding developed in previous work on Si.[4] The capacitance is that between gate and back contacts. The sample is exposed to room-temperature thermal radiation, so that adequate majority-carrier conductivity in the bulk is guaranteed. Band-gap radiation on the sample can be applied with a light-emitting diode (LED) mounted near the sample. At the top of the cryostate visible radiation is blocked with a black polyethylene filter. This arrangement has proved satisfactory to measure the C-V curves at 4.2 K of the $N_{D,A} \sim 2 \times 10^{14}$ cm^{-3} samples.

Typical of the C-V curves for a "good" sample, i.e., one that shows good conductivity and Shubnikov–de Haas oscillations, is that in Fig. 2. The sweep starts at -200 V, which is as high a voltage as can be applied without risking breakdown. Modulation is 1 V p-p at 13 Hz. The capacitance at -200 V is that of the lacquer layer, $C_i \approx 150$ pF. When V_g is swept to positive values, C decreases along the curve marked (1). It follows the relation

$$C(V)/C_i = [1 + \text{const}\ (V - V_{FB})]^{-1/2}$$

as indicated by the dots.[5] From the fit we identify $V_{FB} = -130$ V and the constant is that for $N_A - N_D = 2.0 \times 10^{14}$ cm^{-3}.

For low T the onset of the capacitance decrease at V_{FB} is expected to be sharp. The rounding in Fig. 2 is probably an indication of inhomogeneities across the sample surface. The fact that V_{FB} is negative indicates a sizable positive charge on the "as-prepared" surface.

The depletion charge in equilibrium is calculated as

$$N_{dep} = (|N_A - N_D| E_g \epsilon / 2\pi e^2)^{1/2} = 5 \times 10^{10}\ \text{cm}^{-2}$$

for the proper dielectric constant ϵ and gap energy E_g. Accordingly, V_T is expected to be near -120 V. We realize that the continued drop of C along (1) represents a nonequilibrium situation in which the depletion layer grows to a length far in excess of the equilibrium value 2.5×10^{-4} cm. The obvious reason is the lack of minority carriers. When we reach $V = 0$, the depletion charge is 3.8×10^{11} cm^{-2} and the voltage drop across the depletion layer is ~ 40 V!

There is an abrupt increase of C near $+30$ V. Branch (1) reaches a value of C near the expected equilibrium value. From the value $C/C_i = 0.84$ one calculates $N_A - N_D = 2.5 \times 10^{14}$ cm^{-3}. It is remarkable that after this value of 0.84 C_i has been reached minority carriers appear in the surface layer without band-gap light or a large avalanche voltage across the depletion layer. A likely reason is that the positive interface charge (remember $V_{FB} = -130$ V) provides a surface conductivity channel from the back contact to the gate area. We argue that once the surface layer has been sufficiently charged with minority carriers in an avalanche process (near $V \sim 0$) to become conducting, the entire layer can be supplied with minority carriers via the surface path.

Whatever this source of minority carriers, it is sufficient to supply the required charge in a very slow sweep to more positive V. The part of the curve $+50 \leq V_g \leq 200$ V is perfectly reversible when swept slowly. For a fast sweep rate C is decreased in the up-sweep (1) and increased for the down-sweep (2), because minority carriers are not supplied quickly enough. This is evident also in the V_{mod} dependence of C. At 13 Hz and $V_{mod} = 1$ V a minimum value of C is found. Decreasing the modulation frequency or increasing V_{mod} to 5 or 10 V increases C.

The reverse trace (2) coincides with (1) only to somewhere near where we postulated the onset of

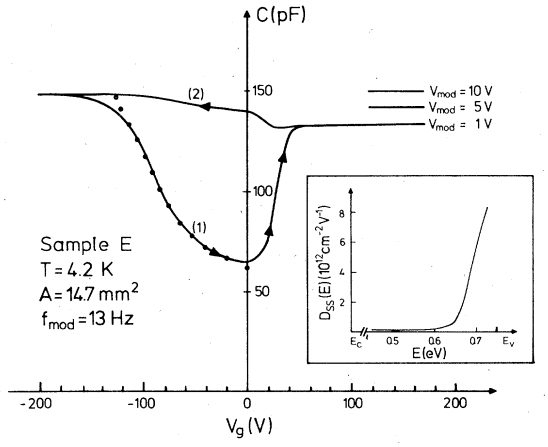

FIG. 2. Hysteretic C-V curve observed on Ge M-I-S capacitors at low temperature. The insert gives the density of interface states obtained from an analysis of the part of the sweep labeled (2).

conduction. Thereafter, a rise of C signals the decrease of the depletion length. The depletion charge is removed via recombination with majority carriers. The long gentle rise of C, the large voltage span to V_{FB}, is an indication of a similar discharging of an interface layer of minority charges. The form of the C-V curve identifies these negative charges to lie mainly in the lower half of the band gap in ionized acceptor-like states. These surface acceptors have been charged in sweep (1) when minority carriers became available in avalanche processes ($-20 \leq V_g \leq +20$ V). In an insert to Fig. 2 the energy distribution of the interface states $D_{ss}(E)$ determined from the form of the C-V curve is shown. The total number of states $N_{ss} = 8 \times 10^{11}$ cm^{-2}.

The capacitance curves serve us as an indicator of sample quality and give an approximate measure of flat-band and threshold voltages. They also point to the existence of a large number of interface states. With the limited breakdown voltage of the lacquer layer this means that only a small maximal inversion layer density can be reached, in Fig. 2 $N_{s\,max} \approx 1 \times 10^{12}$ cm^{-2}. In order to increase this number, we have learned to make use of a gate-bias voltage technique. When cooling from 300 and 77 K, a large negative gate voltage is applied for a number of hours. The sample is cooled to 4.2 K with this bias applied. In this way the onset of conduction can be moved far over to negative voltages. An effective inversion layer density of more than 2×10^{12} cm^{-2} can be achieved in this way. We find that the conductivity of the inversion charge is not much altered by the existence of this extra bias charge layer near the interface.

There are differences and variations in details of the C-V curves from sample to sample. By and large, however, the behavior described above is typical not only of the (111) surface, but also of the (100) and (110) surfaces that we have prepared in a similar way.

IV. SURFACE CONDUCTIVITY

The C-V curve indicates the presence of charges in the surface layer. Their conductivity is registered in the microwave spectrometer.[2,3] The usual arrangement is such that capacitance and conductivity, either $\sigma(V_g)$ directly or its derivative $d\sigma/dV_g$, can be recorded simultaneously. A side-by-side comparison of the two quantities is instructive.

Figure 3 shows a C-V curve and its related conductivity. There is an interesting and relevant difference in C compared to the previous case. The capacitance reaches a constant minimum value in the up-sweep (broken line in Fig. 3). In this part of the curve minority carriers are generated by avalanche breakdown and reach the surface. $\sigma(V_g)$, however,

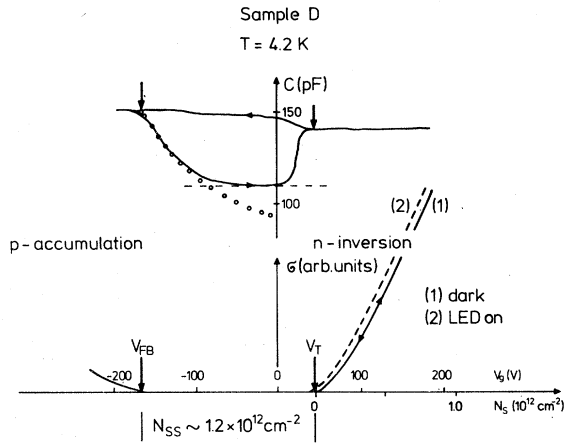

FIG. 3. Correlated C-V and conductivity curves. The capacitance plateau indicated by the broken line is evidence for avalanche breakdown in this sample. LED: light-emitting diode.

remains zero until a voltage just after the sharp rise of C has been reached. The onset of conductivity at V_T relates to the point where the up-down sweeps of C first separate. At negative V_g we mark the onset of accumulation conductivity at V_{FB}, which coincides nicely with the square-root fit. The conductivity curve, in contrast to the hysteretic $C(V)$, is perfectly reversible. The interface charge N_{ss} for the sample in Fig. 3 is 1.2×10^{12} cm^{-2}.

The effect of light on the electron signal is indicated by the dashed curve that appears displaced to the left. For the $N_A - N_D \sim 10^{14}$ cm^{-3} samples the shift is about 10 V and corresponds to the magnitude of the depletion charge. We must assume that the light leads to a nonequilibrium quasiaccumulation condition. The C-V curve is radically changed by the light and can no longer be interpreted easily. The conductivity curve for both types of samples, except for the horizontal displacement, is not affected.

The conductivity in Fig. 3 can be followed only to small N_s because of breakdown-limited V_g. The use of mylar foils allows a larger N_s value to be reached, but has two distinct disadvantages, because it is not integrally bonded to the surface. One finds always spurious signals from foil movement, and sample surfaces are unstable and tend to "corrode" with time. As Fig. 4 shows, the sweep can be continued to $\sim 5 \times 10^{12}$ cm^{-2} and thus gives a better impression of the overall conductivity. Typically the ratio of electron to hole mobilities is ~ 4. A linear rise of σ is found up to $N_s \sim 1 \times 10^{12}$ cm^{-2}. Thereafter the slope decreases considerably. The microwave measurements are not in terms of absolute units, and it is impossible to compare directly the two types of samples. The foil-type, naked surfaces generally have larger N_{ss}, here 2.1×10^{12} cm^{-2}.

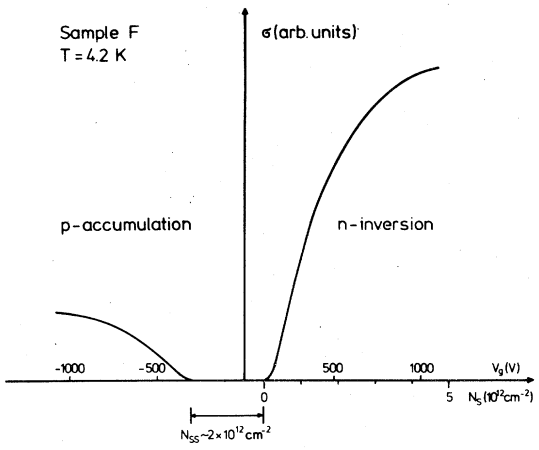

FIG. 4. Conductivity curve for a foil-type sample. Note the large value of N_{ss} and the decreasing slope above $N_s \sim 1 \times 10^{12}$ cm^{-2}.

The difficulty of small maximal N_s on the lacquer samples is remedied by the gate-bias technique mentioned in Sec. III. It has proved possible to move the onset of conduction to negative voltages near breakdown, and thus double the effective maximum value of N_s. The procedure has no detrimental effect on the conductivity.

A critical comparison of samples is made with the $d\sigma/dV_g$ curves in Fig. 5. These field-effect mobility curves are a sensitive indicator of the N_s dependence of scattering in the surface layer. The curves have been adjusted to coincide in the height of the first maximum. Samples *A*, *B*, and *C* are all lacquer-coated (111) specimens prepared at various times. *F* is a foil-covered (111) sample. It is a common property of the foil samples that $d\sigma/dV_g$ decreases notably with rising N_s. Some lacquer specimens (sample *C*) show a similar effect. Others, such as *A* and *B*, have high mobilities out to maximal N_s. These two samples have given the best magneto-oscillation data at high N_s. For sample *A* the second $d\sigma/dV_g$ peak coincides with the growth of the "extra" structure referred to in the Introduction.

Data such as those cited in Figs. 3–5 have been obtained also for (100) and (110) planes of Ge. The results closely follow those for the (111) specimens. A quantitative comparison of surface conductivity on these planes, however, is not possible with the present microwave system.

In order to get a measure of the relaxation time τ and to select the best specimen for the magneto-oscillation studies, we examine σ in a perpendicular magnetic field. The expected variation of σ with H is

$$\sigma_{xx}(H) = \frac{\sigma_{xx}(0)}{1+\omega_c^2\tau^2} \quad , \tag{1}$$

for a homogeneous group of carriers with cyclotron frequency ω_c. The comparison in Fig. 6 is typical for (110), (100), and (111) surfaces. For the first two curves, $N_s \sim 1.4 \times 10^{12}$ cm^{-2} is near the maximum in $d\sigma/dN_s$ for the samples. Making use of the appropri-

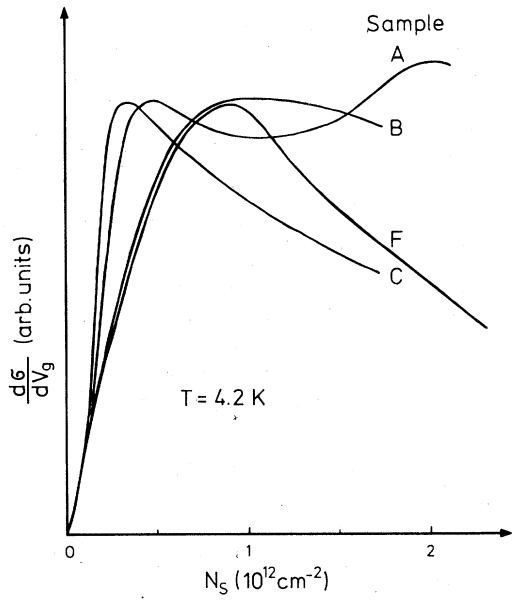

FIG. 5. Field-effect mobility curves vs N_s for a number of differently prepared and treated specimens. The heights have been adjusted to agree at the first maximum.

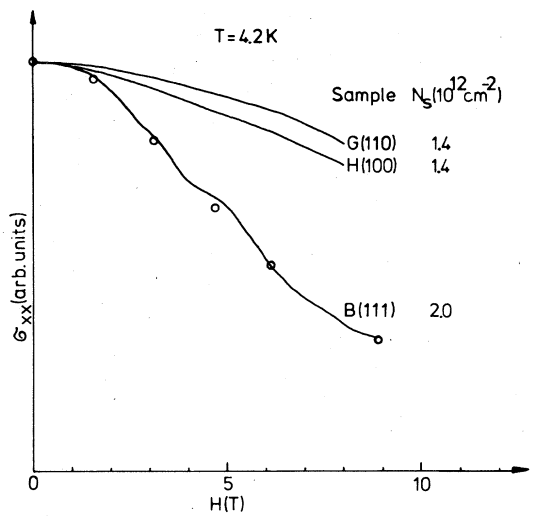

FIG. 6. Electron conductivity $\sigma_{xx}(H)$ in a perpendicular magnetic field for different planes. Each of the three curves can be fitted satisfactorily to Eq. (1) in the text and for the relaxation times quoted there. The open circles on the (111) curve are for a two-carrier description with the measured densities.

ate cyclotron masses[6] we find the relaxation times

$$\tau_{(100)} = 1.1 \times 10^{-13} \text{ sec} ,$$

$$\tau_{(110)} = 0.75 \times 10^{-13} \text{ sec}$$

and

$$\tau_{(111)} = 0.8 \times 10^{-13} \text{ sec}$$

for the curves in Fig. 6.

The relaxation times for the three surfaces are similar, but only for the (111) specimen do we reach the condition $\omega_c \tau > 1$ in the available range of H. For the (111) surface we expect, and do find (cf. Fig. 1), well-resolved conductivity oscillation. A comparison of Figs. 1 and 6 raises an interesting question. In Fig. 1 distinct oscillations persist to $H \sim 2$ T, where with the $\tau_{(111)}$ from Fig. 6 they should no longer be observable. An analysis of the collision damping of the oscillations gives $\tau = 1.6 \times 10^{-13}$ sec (Sec. V). The discrepancy could be resolved, if one assumed the curve in Fig. 6 to contain a major contribution from an additional low-mobility carrier. Could this be the missing 80% of induced charge?

V. SHUBNIKOV–de HAAS EFFECT AND SUBBAND OCCUPATIONS

With the appearance of extra structure in Fig. 1 we have raised the question of additional occupied subbands on the (111) surface. To identify a possible new period it was necessary to make use of higher H fields. Such measurements were carried out in the 14.6-T coil of the University of Würzburg laboratory. The sequence of traces in Fig. 7 allows us to identify the oscillations of two different periods, S_0 and S_1.

We complement the high-field, high-N_s data with traces for lower N_s ($H < 10$ T) in Fig. 8. Together the curves show how well the various peaks can be identified and followed for the range of N_s accessible in a lacquer-type sample. The earlier work,[1] as well as our present efforts with foil-covered (111) surfaces, never gave any indication of the period S_0.

We assume spin degeneracy ($g_s = 2$) and associate the oscillations with the nondegenerate valley, i.e., $g_v = 1$. The occupancies of the subbands, N_s^n, are then determined according to

$$N_s^n = \frac{g_s g_v}{2\pi\hbar} \frac{e}{\Delta(1/H)_n} , \tag{2}$$

with $\Delta(1/H)_n$ equal to the period in reciprocal field for the series of oscillation peaks S_n. The values N_s^0 and N_s^1 are entered in Fig. 9 as a function of the induced charge measured from the conduction threshold at V_T. From data on foil-type samples the occupancy N_s^1 is continued out to $N_s = 3.5 \times 10^{12}$ cm^{-2} in Fig. 9. The occupation N_s^1 coincides with values obtained in Ref. 1 up to a maximum N_s in Fig. 9. Reference 1 gives an N_s^1 that continues linearly with N_s out to 6.2×10^{12} cm^{-2} of induced charge. Where there are no vertical error bars marked, the estimated uncertainty does not exceed the size of the point drawn in Fig. 9. The large error bars on some of the N_s^0 values reflect the considerable uncertainty in locating the weak oscillations. The period S_1 cannot be followed to below 1.3×10^{12} cm^{-2}, because only a single peak (lowest Landau level) remains (see Fig. 8).

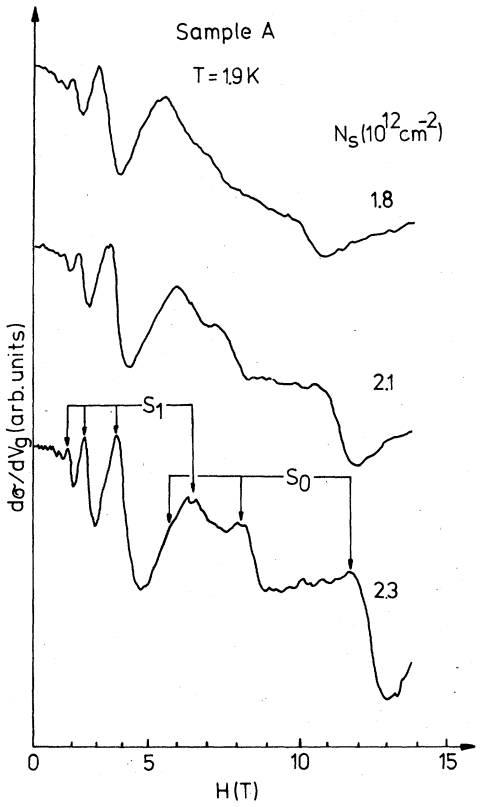

FIG. 7. Magneto-oscillation spectrum of (111) Ge. S_0 and S_1 are series of peaks associated with the ground state and the next higher-lying subband.

The magneto-oscillations were observed in both n- and p-type samples with $N_{A,D} \sim 10^{14}$ cm^{-3}, and in the high-purity $N_{A,D} \sim 10^{11}$ cm^{-3} material. In each case the periods as shown in Fig. 9 were obtained. The oscillations also were not changed with band-gap illumination of the surface, except for the shift in V_T.

The solid line without the experimental points in Fig. 9 is N_s itself. It should be equal to the sum of all the subband occupancies. A possible error in the determination of V_T must be considered as an uncertainty in the lateral position of this line relative to the N_s^n. Such an estimated error is marked with horizontal error bars. Its absolute slope is by definition 1.

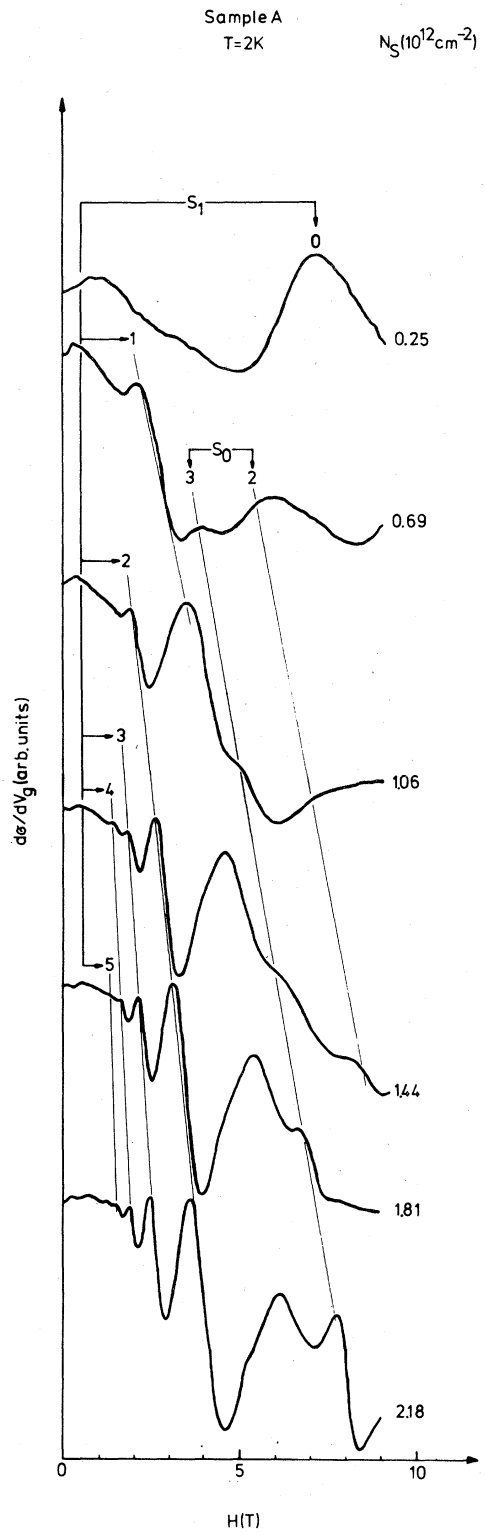

FIG. 8. Magneto-oscillations and their identification over the entire range of occupation density.

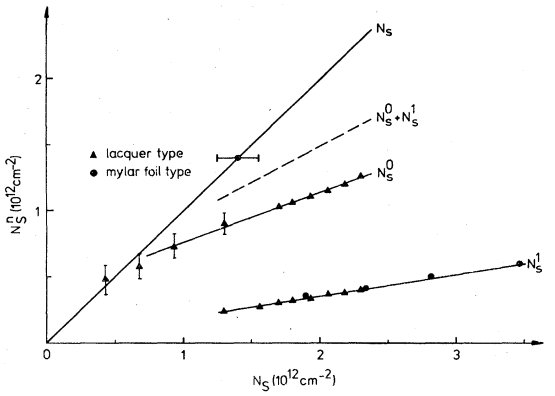

FIG. 9. Occupations N_s^0 and N_s^1 from the measured periods. N_s^1 has been measured in both lacquer-coated (▲) and foil-covered (●) samples. The occupation N_s^1 continues to rise linearly with the same slope out to $N_s = 6.2 \times 10^{12}$ cm^{-2}.

Relative to the lines N_s^n its slope is uncertain only to the uncertainty of the capacitance measurement, which is negligibly small.

The sum $N_s^0 + N_s^1$ appears as a broken line in Fig. 9 over the range of N_s where both periods have been observed. This sum must be compared with the line N_s. Within the given uncertainties the sum $N_s^0 + N_s^1$ can account reasonably for the total occupation up to $N_s \sim 1 \times 10^{12}$ cm^{-2}. After $N_s = 1.3 \times 10^{12}$ cm^{-2} the difference becomes so large that we can with certainty state that the total carrier density is greater than $N_s^0 + N_s^1$.

We obtain also from the oscillations an approximate measure of the relaxation time τ. For fields and temperatures such that $2\pi^2 kT/\hbar\omega_c < 1$, the amplitude of the oscillations vanishes as $e^{-\pi/\omega_c\tau}$. This case of collision damping is satisfied for example in Fig. 1 near 2 T. A plot of ln of the amplitude versus $1/H$ gives $\tau = 1.6 \times 10^{-13}$ sec^{-1} for the S_1 period that appears in Fig. 1 for the lacquer-type sample.

We have searched for magneto-conductivity oscillations in the (100) and (110) plane samples at $T \sim 1.2$ K up to 9.5 T and for the usual range of densities N_s. As one would expect from the discussion of the $\sigma_{xx}(H)$ curves in Fig. 6, no oscillations were identified.

VI. DISCUSSION

The present work has provided clear evidence for the occupancy of two or more subbands on (111) Ge and thus provides the answer to the question raised in Ref. 1 regarding the "missing" electrons. The answer to why the S_0 period was not observed previously lies in the surface preparation. The curves in Fig. 5 show that the naked, foil-type samples have a

marked decrease in mobility with rising N_s. At N_s values where S_0 is found in the other samples, $d\sigma/dV_g$ has decreased to about one-half maximum value.

It is expected to find that the S_1 oscillations persist to N_s values where S_0 has disappeared. We suggest that the high density of interface charge N_{ss} is the reason. The smaller binding length of the ground-state subband results in stronger interaction and scattering. When charged, impurity scattering predominates. In particular for low N_s one would have $\tau_0 < \tau_1$. It is interesting to note that for sample A the rise and second maximum of $d\sigma/dV_g$ (cf. Fig. 5) coincides with the growth of the period S_0.

With such multiple-subband analysis of the conductivity we must reconsider $\sigma_{xx}(H)$ in Fig. 6. We had noted that the (111) curve corresponded to a τ value 0.8×10^{-13} sec, if fitted to Eq. (1). If instead we insist to fit with two carrier contributions according to the N_s^0 and N_s^1 in Fig. 9, the necessary τ values are $\tau_0=0.6\times10^{-13}$ sec and $\tau_1=1.3\times10^{-13}$ sec. The points indicated on the curve are for these values. The τ values are approximate, because we ignore the fact that $N_s^0+N_s^1$ is not equal to N_s. Nevertheless, the numbers confirm our supposition $\tau_1 > \tau_0$.

When we compare the (111) and (100) and (110) surfaces, we realize that it is the low density of states in the subband which for the (111) plane favors the filling of a higher level with its good value of τ. With $g_v=4$ and $m_c^*=0.30m_0$ the (100) plane subbands have $\sim$14 times the density of states. For the (110) plane the factor is $\sim$6 for $m_c^*=0.22m_0$ and $g_v=2$. For both of these planes it is unlikely that anything but the ground state is occupied.

If this is so, the $\tau_{100}=1.1\times10^{-13}$ sec quoted in Sec. IV belongs to this ground state. The point $\omega_c\tau\sim1$ is reached at $\sim$15 T. At this field, for $N_s=2.0\times10^{12}$ cm^{-2}, most carriers would occupy the lowest Landau level. No oscillation would be expected out to our highest fields.

A corresponding check for the (110) samples with $\tau_{110}=0.75\times10^{-13}$ sec leads us to expect oscillations above the $\omega_c\tau\sim1$ point of $\sim$13 T. At this field less than two Landau levels are filled. With the 20-T field there would have been a chance to identify sufficient structure to obtain a period in such a sample. For the present state of the art of surface preparation and the fields H available in this experiment, it is not expected that useful magneto-oscillation data could be obtained in (100) and (110) samples. It is primarily the occupation of a higher subband in (111) plane specimens that has allowed the successful work in this surface.

From the experimental observations we can reach a number of conclusions related to the subband energy structure of the (111) surface. Since both n- and p-type samples ($N_A, N_D\sim10^{14}$ cm^{-3}), or for that matter the high-purity samples, give the same periods and occupations we conclude that for the relevant range of N_s the depletion charge potential can be ignored. A guess for the relative ordering of subbands comes from a triangular-well calculation. The lowest three bands are then $n=0,1,2$ states of the nondegenerate valley. There follows the threefold degenerate 0′ level just above $n=2$.

The experimental evidence in Fig. 9 is for occupied $n=0$ and 1 levels that increase their occupancy linearly with N_s. The fact that no period S_2 appears, even though the sum $N_s^0+N_s^1$ comes to fall substantially below N_s, can only mean that 0′ with its $\sim$12 times higher density of states is being filled and lies close in energy to the $n=2$ level. According to the plot, a third level is being filled above $N_s=1.0\times10^{12}$ cm^{-2}. If this were the $n=2$ level only, it should be observable as a distinct third period, at least above $N_s\sim1.5\times10^{12}$ cm^{-2}.

If instead we assign the missing charge primarily to 0′ occupation, it is clear why no new oscillations appear. The cyclotron mass for these $g_v=3$ electrons is $m_c^*=0.34m_0$. With $\tau_{0'}=\tau_1$ we can scale up the observations of the S_1 period to predict that $S_{0'}$ should occur only at fields above 8 T. At this field, however, the entire missing charge of 0.6×10^{12} cm^{-2} at $N_s\sim2.3\times10^{12}$ cm^{-2} would only half fill the lowest Landau level.

With the observed periods S_0 and S_1 and the known $m_c^*=0.08m_0$ we can construct the subband energy separation $\epsilon_1-\epsilon_0=\epsilon_{01}$ with N_s^0 and N_s^1 increase linearly with N_s. It follows that ϵ_{01} increases linearly from 18.6 meV at 1.3×10^{12} cm^{-2} to 24.8 meV at 2.3×10^{12} cm^{-2}. This provides the first experimentally based determination of subband splittings in Ge.

VII. CONCLUDING REMARKS

The experimental work, in particular the detailed results on (111) Ge, has prompted a theoretical analysis of the subband energies and occupations. The results are contained in Paper II (see Ref. 7).

ACKNOWLEDGMENTS

We acknowledge many interesting discussions with B. Vinter. The work with the high-field magnet in Würzburg was important to confirm and accurately determine the S_0 period. We want to thank K. v. Klitzing for participating in this part of the work. Financial support for the investigation was provided by the Deutsche Forschungsgemeinschaft under SFB 128. K. Germanova participated in this project with the sponsorship of the Humboldt foundation.

*Based on a doctoral thesis submitted in partial fulfilment of the requirements for the degree Dr.rer.nat. at Technische Universität München.

†Permanent address: Phys. Dept. Univ. of Sofia, Bulgaria.

[1]W. Weber, G. Abstreiter, and J. F. Koch, Solid State Commun. 18, 1397 (1976).

[2]J. F. Koch, in *Advances in Solid State Physics XV,* edited by H. J. Queisser (Pergamon, New York, 1975), p. 79.

[3]J. F. Koch, Surf. Sci. 58, 104 (1976).

[4]P. Kneschaurek, A. Kamgar, and J. F. Koch, Phys. Rev. B 14, 1610 (1976).

[5]See, for example, S. M. Sze, *Physics of Semiconductor Devices* (Wiley, New York, 1969), Chap. 9.

[6]F. Stern and W. E. Howard, Phys. Rev. 163, 816 (1967).

[7]J. Binder, A. Huber, K. Germanova, and F. Koch, Phys. Rev. B 20, 2391 (1979) (following paper).